

Reheating constraints on Tachyon Inflation

Akhilesh Nautiyal

*Department of Physics, Malaviya National Institute
of Technology Jaipur, JLN Marg, Jaipur-302017*

Abstract

Tachyon inflation is one of the most attractive models of noncanonical inflation motivated by string theory. In this work we revisit the constraints on tachyon inflation with inverse cosh potential and exponential potential considering reheating. Although the phase of reheating is not well understood, it can be parameterized in terms of reheating temperature T_{re} , number of e-folds during reheating N_{re} and effective equation of state during reheating w_{re} , which can be related to the parameters of the tachyon potential, spectral index n_s and tensor-to-scalar ratio r . For various reheating scenarios there is a finite range of w_{re} and the reheating temperature should be above electroweak scale. By imposing these conditions, we find that both the inverse cosh potential and exponential potential are disfavored by Planck observations. We also find that w_{re} for both these potentials should be close to 1 to satisfy Planck-2015 joint constraints on n_s and r .

PACS numbers: 98.80.Cq, 14.80.Va, 98.80.-k, 98.80.Qc

1. INTRODUCTION

Inflation [1] not only provides solution to the problems of big bang cosmology, but also generates seeds for CMB anisotropy and structures in the universe [2–4]. It predicts adiabatic, nearly scale invariant and Gaussian perturbations which are confirmed by various CMB observations like COBE [5], WMAP [6] and Planck [7]. In standard scenario the potential energy of a scalar field, named as inflaton, dominates the energy density of universe for a short period of time that causes the rapid expansion of the universe. The inflaton field ϕ , whose dynamics can be determined by the Klein-Gordon action, rolls slowly through its potential. During this period the quantum fluctuations in the scalar field, which are coupled to the metric fluctuations, generate the primordial density perturbations. There are also vacuum fluctuations of the metric during inflation that generate primordial gravitational waves (tensor perturbations). The power spectra of the primordial density perturbations and tensor perturbations generated during inflation depend on the potential of the inflaton, which can be obtained from particle physics models or string theory.

There are some alternative to the standard inflationary models [8, 9], named as K-inflation, where the inflation is achieved by non-standard kinetic term in the Lagrangian of the inflaton. One attractive and popular model of K-inflation is tachyon inflation [10], which can be realized in Type-II string theory where the tachyon signals the instability of unstable and uncharged D-branes of tension λ . In this case the tachyon action is of the Dirac-Born-Infeld form (see [11–17] for different approaches). It was also pointed out by Sen [18] that the rolling tachyon can have the dust like equation of state, which raised the possibility of tachyon providing a unified description of inflation and dark matter. However, tachyon as inflaton has been criticized in [19, 20] as the string theory motivated values of the parameters are incompatible with the slow-roll conditions and observed amplitude of the scalar perturbations. Despite the criticism and regardless the string theory motivation, tachyon inflation has been studied phenomenologically as an example of noncanonical inflation model [21, 22]. In [21] it was shown that the consistency relation in case of tachyon inflation is different than the standard single field inflation and an observational signature of this deviation can lead to distinguish between the two models.

Inflation leaves the universe in a cold and highly nonthermal state without any matter content. Universe needs to be in a thermalized state at a very high temperature for hot big bang picture. This is achieved by reheating which is a transition phase between the end of inflation and the start of radiation dominated era. During reheating the energy density of inflaton is converted to the thermal bath, at a reheating temperature T_{re} , that fills the universe at the beginning of radiation dominated era (see [23] for detailed review). In simplest case reheating can occur via perturbative decay of inflaton into standard model matter particles, while inflaton is oscillating around the minimum of its potential [24–26], but this scenario was criticized in [27, 28] as it does not take into account the coherent nature of the inflaton field. In other scenarios reheating is preceded by phase of preheating during which the particle production occurs via non-perturbative processes such as parametric resonance decay [29, 30], tachyonic instability [31, 32] and instant preheating [33]. Preheating leaves the universe in highly nonthermal state which is thermalized by scattering and the universe is left with a blackbody spectrum at a temperature T_{re} , named as reheating temperature, which corresponds to the temperature at the beginning of the radiation dominated epoch.

It is difficult to constrain the reheating temperature T_{re} from CMB and LSS observations, but it is considered that T_{re} should be above the electroweak scale: so that the weak scale dark matter can be produced. If we adopt a conservative approach, T_{re} must be greater than 10MeV for the big bang nucleosynthesis. The upper bound on reheating temperature is obtained by assuming reheating to be an instantaneous process which reheats the universe to the scale of inflation i.e. 10^{16} GeV by considering the Planck upper bound on tensor-to-scalar ratio. The evolution of the energy density of the cosmic fluid during reheating depends on effective equation of state w_{re} , which, in general, depends on time. Its value at the end of inflation is $-\frac{1}{3}$ and reaches $\frac{1}{3}$ at the beginning of radiation dominated epoch. In case where the reheating occurs due to perturbative decay of massive inflaton, the effective equation of state during reheating w_{re} is $w_{re} = 0$ and for instant reheating $w_{re} = \frac{1}{3}$. A numerical study performed for various reheating scenario [34] shows that w_{re} can vary between 0 to 0.25. Another important parameter to describe reheating is its duration, which can be defined in terms of number of e-foldings N_{re} from the end of inflation to the onset of radiation dominated epoch. In general, this is incorporated by providing a range for N_k , the number of e-folds from the time when a Fourier mode k corresponding the the horizon size of our observable universe leaves the inflationary horizon to the end of inflation. N_k depends on the potential of inflaton and it should be between 46 to 70 to solve the horizon problem. The upper bound on N_k comes from assuming instantaneous reheating and the lower bound arises from considering reheating temperature at electroweak scale.

These three parameters of reheating can be used to obtain constraints on various inflationary models [35–37]. Demanding that the equation of state during reheating lies between 0 and 0.25, one can get bounds on the spectral index n_s and N_k , which translates to bounds on tensor-to-scalar ratio r . In this work we use this approach to constrain tachyon inflation with inverse cosh and exponential potentials. We obtain T_{re} and N_{re} as a function of spectral index as in [37] by assuming w_{re} to be constant during reheating. We obtain the allowed regions for these potentials in $n_s - r$ plane for various values of w_{re} . We also use Planck-2015 1σ bounds on n_s and r to determine the equation of state during reheating for these potentials.

The work is organized as follows: in Sec. 2 we give a brief review of tachyon inflation providing the expressions for N_k , scalar power spectrum, spectral index n_s and tensor to scalar ratio r . In Sec. 3 we provide the derivation for reheating temperature T_{re} and number of e-folds during reheating N_{re} for constant effective equation of state w_{re} . In Sec. 4 we obtain T_{re} , and N_{re} for tachyon inflation with inverse cosh and exponential potential for various choices of equation of state w_{re} and use these three parameters to constrain tachyon inflation. In Sec. 5 we conclude our work.

2. TACHYON INFLATION

Tachyon inflation is a class of K -inflation models where inflation is achieved by noncanonical kinetic term. the action for tachyon inflation is given by

$$S_T = - \int d^4x \sqrt{-g} V(T) (1 + g^{\mu\nu} \partial_\mu T \partial_\nu T)^{\frac{1}{2}} \quad (1)$$

and the metric has signature $- , + , + , +$. T represents the tachyon field with dimension of length and $V(T)$ represents its potential. Various choice for the potential have been derived using string theory [11–17]. Here we consider the inverse cosh potential [11, 12, 38] and exponential potential [39, 40] given by

$$V(T) = \frac{\lambda}{\cosh\left(\frac{T}{T_0}\right)} \quad (2)$$

and

$$V(T) = \lambda \exp\left(-\frac{T}{T_0}\right) \quad (3)$$

The action for the tachyon-gravity system is given by

$$S = \int d^4x \sqrt{-g} \frac{R}{16\pi G} + S_T \quad (4)$$

The energy-momentum tensor can be obtained by varying this action as

$$T_{\mu\nu} = -V(T)g_{\mu\nu}\sqrt{1 + \partial^\mu T \partial_\mu T} + \frac{V(T)}{\sqrt{1 + \partial^\mu T \partial_\mu T}} \partial_\mu T \partial_\nu T \quad (5)$$

The energy density and pressure for the background part of the tachyon field in a homogeneous and isotropic universe is given as

$$\rho = \frac{V(T)}{\left(1 - \dot{T}^2\right)^{\frac{1}{2}}} \quad (6)$$

$$p = -V(T) \left(1 - \dot{T}^2\right)^{\frac{1}{2}} \quad (7)$$

Hence the Friedmann equation becomes

$$H^2 = \frac{1}{3M_p^2} \frac{V(T)}{\left(1 - \dot{T}^2\right)^{\frac{1}{2}}}, \quad (8)$$

and the equation of motion for the background part of the tachyon field can be obtained using the conservation of energy-momentum tensor as

$$\frac{\ddot{T}}{\left(1 - \dot{T}^2\right)} + 3H\dot{T} + (\ln V)' = 0 \quad (9)$$

The conditions to achieve inflation can be obtained by using Friedmann equation

$$\frac{\ddot{a}}{a} = -\frac{1}{6M_p^2} (\rho + 3p) = \frac{1}{3M_p^2} \frac{V}{\left(1 - \dot{T}^2\right)^{\frac{1}{2}}} \left(1 - \frac{3}{2}\dot{T}^2\right) > 0, \quad (10)$$

which gives $\dot{T}^2 < \frac{3}{2}$. And also for inflation to last sufficiently longer \ddot{T} should be smaller than the friction term in the equation of motion for tachyon field Eq. (9)

$$\ddot{T} < 3H\dot{T} \quad (11)$$

Hence during inflation

$$\dot{T} \sim -\frac{(\ln V)'}{3H}, \quad H^2 \sim \frac{V}{3M_p^2} \quad (12)$$

To analyze the dynamics of inflation the slow-roll parameters can be defined in terms of the Hubble flow parameters [41] as

$$\epsilon_0 \equiv \frac{H_k}{H} \quad (13)$$

$$\epsilon_{i+1} \equiv \frac{d \ln |\epsilon_i|}{dN}, \quad i \geq 0, \quad (14)$$

where H_k is the Hubble constant during inflation when a particular mode k leaves the horizon and N is the number of e-foldings

$$N \equiv \int_t^{t_e} H(t) dt, \quad (15)$$

where t_e is the end of inflation. We also have

$$\dot{\epsilon}_i = \epsilon_i \epsilon_{i+1}. \quad (16)$$

In terms of T the slow-roll parameters defined by Eqs. (13) and (14) can be written as

$$\epsilon_1 = \frac{3}{2} \dot{T}^2 \quad (17)$$

$$\epsilon_2 = \sqrt{\frac{2}{3\epsilon_1}} \frac{\epsilon'}{H} = 2 \frac{\ddot{T}}{H\dot{T}} \quad (18)$$

For conditions 12 to be satisfied, $\epsilon_1, \epsilon_2 \ll 1$ and inflation ends when $\epsilon_1 = 1$.

The power spectra for scalar and tensor perturbations, spectral index and tensor to scalar ratio in these models are given as [9, 21]

$$P_\zeta = \left. \frac{H^2}{8\pi^2 M_p^2 c_S \epsilon} \right|_{c_S k=aH} \quad (19)$$

$$P_h = \left. \frac{2}{\pi^2} \frac{H^2}{M_p^2} \right|_{k=aH} \quad (20)$$

$$n_s = 1 - 2\epsilon_1 - \epsilon_2 \quad (21)$$

$$r = 16c_S \epsilon \quad (22)$$

Here c_S is the effective sound speed given as

$$c_S^2 = \frac{\partial P / \partial \dot{T}^2}{\partial \rho / \partial \dot{T}^2} = 1 - \dot{T}^2 \quad (23)$$

The effective sound speed for these models is very close to 1. The power spectrum P_ζ , spectral index n_s and tensor-to-scalar ratio r are all evaluated at the pivot scale $k = k_0$ which is 0.05Mpc^{-1} for Planck observations. All these parameters depend on the choice of the tachyon potential $V(T)$ and are constrained by CMB and LSS observations. In Sec. 4, we will discuss how reheating can be used to limit our choice of the potentials. Before that we discuss the relation between reheating parameters and inflationary parameters in the next section.

3. REHEATING

Models of reheating can be parameterized in terms of thermalization temperature T_{re} at the end of reheating, duration of reheating N_{re} and equation of state during reheating w_{re} [36, 37]. We consider w_{re} to be constant during reheating and it should be larger than $-\frac{1}{3}$ for inflation to end and should be smaller than 1 to the causality to be preserved.

If the equation of state remains the same during reheating, the change in the scale factor can be related to the change in energy density by using $\rho = a^{-3(1+w)}$ as

$$\frac{\rho_{end}}{\rho_{re}} = \left(\frac{a_{end}}{a_{re}} \right)^{-3(1+w_{re})}. \quad (24)$$

Here the subscripts *end* and *re* denote the values of the quantity at the end of inflation and at the end of reheating respectively. Eq. (24) can be expressed in terms of $N_{re} = \ln \left(\frac{a_{re}}{a_{end}} \right)$ as

$$\begin{aligned} N_{re} &= \frac{1}{3(1+w_{re})} \ln \frac{\rho_{end}}{\rho_{re}} \\ &= \frac{1}{3(1+w_{re})} \ln \left(\frac{3}{2} \frac{V_{end}}{\rho_{re}} \right). \end{aligned} \quad (25)$$

Here we have substituted $\rho_{end} = \frac{3}{2}V_{end}$ as the equation of state at the inflation is $-\frac{1}{3}$. The relation between the reheating temperature T_{re} and N_{re} can be obtained by expressing the energy density at the end of reheating ρ_{re} in terms of T_{re} as

$$\rho_{re} = \frac{\pi^2}{30} g_{re} T_{re}^4. \quad (26)$$

So from Eq. (25) we get

$$N_{re} = \frac{1}{3(1+w_{re})} \ln \left(\frac{30 \cdot \frac{3}{2} V_{end}}{\pi^2 g_{re} T_{re}^4} \right). \quad (27)$$

Using entropy conservation the temperature at the end of reheating can be related to the CMB temperature today as

$$T_{re} = T_0 \frac{a_0}{a_{re}} \left(\frac{43}{11g_{re}} \right)^{\frac{1}{3}} = T_0 \frac{a_0}{a_{eq}} e^{N_{RD}} \left(\frac{43}{11g_{re}} \right)^{\frac{1}{3}}, \quad (28)$$

where T_0 is the CMB temperature today, a_0 is the scale factor today, N_{RD} is the number of e-foldings during radiation dominated epoch and a_{eq} is the scale factor at matter-radiation equality. The ratio $\frac{a_0}{a_{eq}}$ can be expressed as

$$\frac{a_0}{a_{eq}} = \frac{a_0}{a_k} \frac{a_k}{a_{end}} \frac{a_{end}}{a_{re}} \frac{a_{re}}{a_{eq}} = \frac{a_0 H_k}{k} e^{-N_k} e^{-N_{re}} e^{-N_{RD}}, \quad (29)$$

where a_k and H_k are the values of scale factor and the Hubble constant during inflation when the Fourier mode k leaves the horizon, N_k is the number of e-foldings from this time to the end of inflation and $k = a_k H_k$ for horizon exit. Now using Eqs. (29) and (28) the relation between T_{re} and N_{re} can be expressed as

$$T_{re} = T_0 \frac{a_0 H_k}{k} \left(\frac{43}{11g_{re}} \right)^{\frac{1}{3}} e^{-N_k} e^{-N_{re}}. \quad (30)$$

Substituting this into Eq. (27) we obtain the expression for N_{re} as

$$N_{re} = \frac{4}{3(1+w_{re})} \left(\frac{1}{4} \ln \left(\frac{3^2 \cdot 5}{\pi^2 g_{re}} \right) + \ln \left(\frac{V_{end}^{\frac{1}{4}}}{H_k} \right) + \ln \left(\frac{k}{T_0 a_0} \right) + \frac{1}{3} \ln \left(\frac{11g_{re}}{43} \right) + N_k + N_{re} \right). \quad (31)$$

If we consider $w_{re} \neq \frac{1}{3}$, Eq. (31) can be solved to obtain N_{re} as

$$N_{re} = \frac{4}{1-3w_{re}} \left(-\frac{1}{4} \ln \left(\frac{3^2 \cdot 5}{\pi^2 g_{re}} \right) - \frac{1}{3} \ln \left(\frac{11g_{re}}{43} \right) - \ln \left(\frac{V_{end}^{\frac{1}{4}}}{H_k} \right) - \ln \left(\frac{k}{T_0 a_0} \right) - N_k \right). \quad (32)$$

For $w_{re} = \frac{1}{3}$ reheating occurs instantaneously leaving the universe at grand unification scale and hence parameters of reheating cannot be used to constrain models of inflation. Using Eqs. (32) and (30) the temperature at the end of reheating T_{re} can be expressed as

$$T_{re} = \left(\left(\frac{43}{11g_{re}} \right)^{\frac{1}{3}} \frac{a_0 T_0}{k} H_k e^{-N_k} \left(\frac{3^2 \cdot 5 V_{end}}{\pi^2 g_{re}} \right)^{-\frac{1}{3(1+w_{re})}} \right)^{\frac{3(1+w_{re})}{3w_{re}-1}}. \quad (33)$$

The main results of this section are expressions for reheating temperature T_{re} Eq. (33) and number of e-folds during reheating Eq. (32) that depend on the inflationary parameters H_k , N_k and V_{end} . In next section we obtain these parameters for tachyon inflation with inverse cosh and exponential potential in terms of amplitude of scalar perturbations A_s and spectral index n_s . With this T_{re} and N_{re} can be expressed as function of n_s and are used to constrain tachyon inflation by demanding w_{re} between $-\frac{1}{3}$ and 1.

4. CONSTRAINTS ON TACHYON INFLATION

In this section we constrain tachyon inflation with inverse cosh (2) and exponential (3) potential from reheating. To simplify our calculations we define $x \equiv \frac{T}{T_0}$ and a constant dimensionless ratio $X_0^2 \equiv \frac{\lambda T_0^2}{M_{pl}^2}$.

4.1. Inverse cosh potential

The inverse cosh potential (2) can be obtained from string theory [11, 12, 38] and is the most popular choice for tachyon potential. In terms of x it can be written as

$$V = \frac{\lambda}{\cosh x} \quad (34)$$

The two slow-roll parameters ϵ_1 and ϵ_2 for this model can be obtained using Eq. (12), Eq. (17) and Eq. (18) as

$$\epsilon_1 = \frac{1}{2X_0^2} \frac{\sinh^2 x}{\cosh x} \quad (35)$$

$$\epsilon_2 = \frac{1}{X_0^2} \frac{\cosh^2 x + 1}{\cosh x} \quad (36)$$

We can obtain the value of the tachyon field at the end of inflation by putting $\epsilon_1 = 1$ and it gives

$$\cosh x_{end} = X_0^2 + \sqrt{X_0^4 + 1}, \quad (37)$$

which gives $x_{end} = \ln 4X_0^2$ for $X_0 > 1$. The number of e-foldings N_k during inflation from the time when mode k leaves the horizon to the end of inflation can be obtained using Eqs. (15) and (12) as

$$\begin{aligned} N_k &= \int_{t_k}^{t_{end}} H(t) dt = \int_{T_k}^{T_{end}} \frac{H}{T} dT \\ &= -\frac{1}{M_p^2} \int_{T_k}^{T_{end}} \frac{V^2}{V'} dT, \end{aligned} \quad (38)$$

which for the inverse cosh potential becomes

$$N_k = X_0^2 \int_{x_k}^{x_{end}} \frac{1}{\sinh x} dx = X_0^2 \ln \left(\frac{\tanh \frac{x_{end}}{2}}{\tanh \frac{x_k}{2}} \right) \quad (39)$$

Using Eq. (37) and $X_0 > 1$ it can be shown that $\tanh x_{end} \sim 1$ so the value of tachyon field at the time when mode k leaves the inflationary horizon can be given as

$$\tanh \frac{x_k}{2} = e^{-\frac{N_k}{X_0^2}}. \quad (40)$$

From Eq. (40) we obtain

$$\sinh x_k = \frac{1}{\sinh \left(\frac{N_k}{X_0^2} \right)}, \quad \cosh x_k = \frac{1}{\tanh \left(\frac{N_k}{X_0^2} \right)}. \quad (41)$$

The scalar power spectrum P_ζ (19), spectral index n_s (21) and tensor-to-scalar ratio (22) are evaluated at the horizon crossing $c_{sk} = aH$ for pivot scale $k = k_o$, which we choose

0.05Mpc^{-1} as in Planck. P_ζ at k_0 is equal to the amplitude of scalar perturbations A_s so we can express the Hubble constant H_k using Eq. (19) as

$$H_k = \pi M_p \sqrt{8A_s \epsilon_1 c_S}. \quad (42)$$

The spectral index (21) for the potential Eq. (34) can be obtained using Eqs. (35) and (36) as

$$n_s = 1 - \frac{2}{X_0^2} \cosh x_k. \quad (43)$$

The tachyon potential at the end of inflation can be obtained as

$$V_{end} = \frac{\lambda}{\cosh x_{end}} = 3M_p^2 H_k^2 \frac{\cosh x_k}{\cosh x_{end}} \quad (44)$$

Using Eqs. (12,37,43) we get

$$V_{end} = \frac{3}{4} M_p^2 H_k^2 (1 - n_s). \quad (45)$$

We can also write N_k in terms of n_s using Eqs. (41) and (43) as

$$N_k = X_0^2 \tanh^{-1} \left(\frac{2}{X_0^2 (1 - n_s)} \right). \quad (46)$$

Both the slow-roll parameters and c_S can be expressed in terms of spectral index n_s and so the Hubble constant H_k can also be expressed in terms of n_s as

$$H_k = 2\pi M_p \frac{1}{X_0} \sqrt{A_s \left(\frac{\frac{1}{2}(1 - n_s)}{X_0^2} - \frac{2}{(1 - n_s) X_0^2} \right) \left(1 - \frac{\frac{1}{2}(1 - n_s) X_0^2 - \frac{2}{(1 - n_s) X_0^2}}{6X_0^2} \right)} \quad (47)$$

It can be seen from Eqs. (45,47,46) that V_{end} , H_k and N_k are all expressed in terms of amplitude of scalar perturbations A_s and spectral index n_s . Hence T_{re} and N_{re} can be obtained as a function of A_s and n_s by putting these expressions in Eqs. (32) and (33). We use Planck-2015 values [7] for $A_s = 2.20 \times 10^{-9}$ (central value) and $n_s = 0.9645 \pm 0.0049$ for our analysis. The small error bars on A_s does not affect the results.

Fig. 1 shows the variation of temperature at the end of reheating T_{re} and the number of e-folds during reheating N_{re} as a function of spectral index n_s . We chose four values of w_{re} between $-\frac{1}{3}$ to 1. The curves for all w_{re} meet at a point that corresponds to $w_{re} = \frac{1}{3}$, which is defined as instant reheating ($N_{re} \rightarrow 0$). The curve of $w_{re} = \frac{1}{3}$ would pass through this point and be vertical. As depicted in the figure for $X_0 = 7$ the values of T_{re} and N_{re} , for all choices of w_{re} , completely lie outside the Planck bounds on n_s . So to satisfy the observations $X_0 > 1$, which justifies our assumption used in our calculations. We chose physically plausible values for w_{re} i.e. $0 \leq w_{re} \leq 0.25$ obtained in [34] and demand that the reheating temperature T_{re} should be larger than 100GeV (shown by light purple region in Fig. 1) for production of weak scale dark matter. This gives bounds on n_s which are stronger than the Planck 1σ bounds (shown by light pink region in Fig. 1) for large value of X_0 . These bounds on n_s correspond to the bounds on N_k , which can be obtained using Eq. (46) and are listed in Table I.

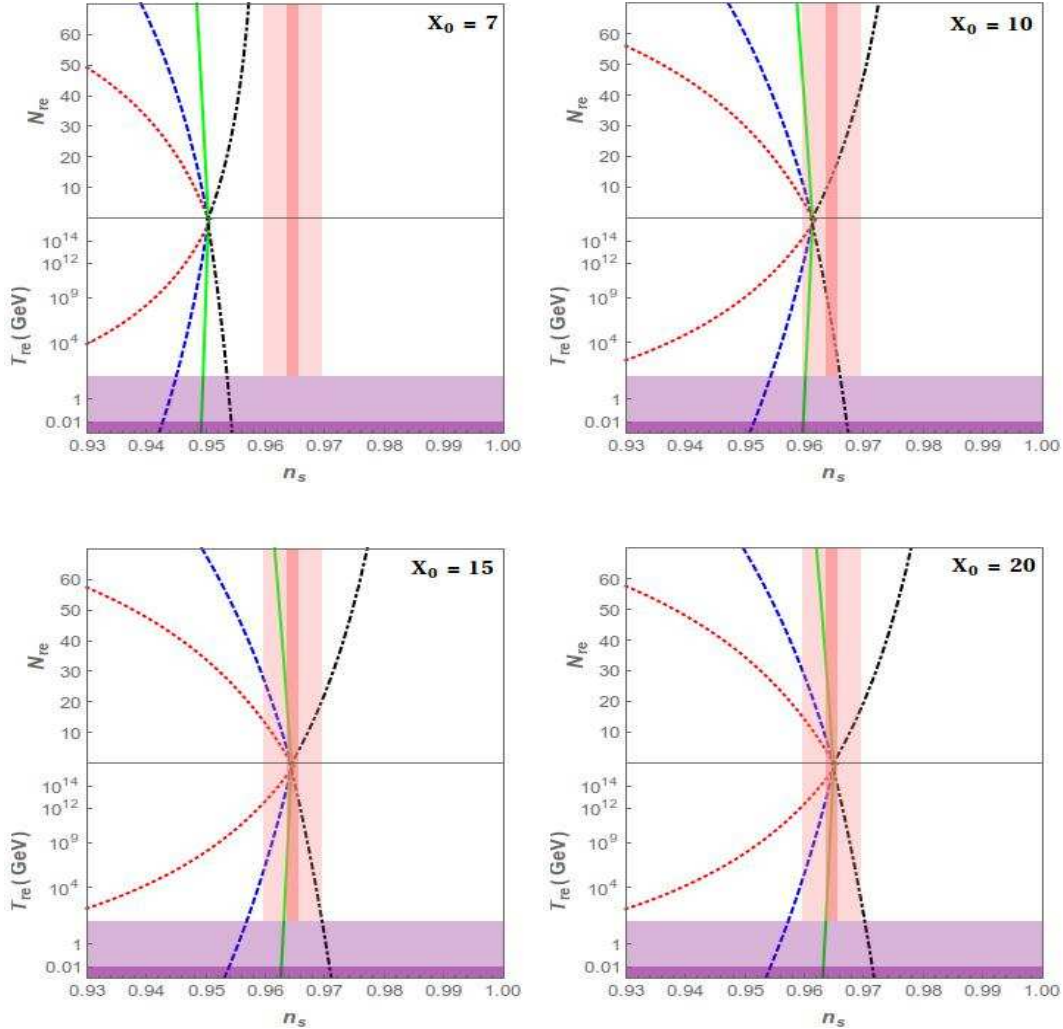


FIG. 1: Figure shows N_{re} and T_{re} , the length of reheating and temperature at the end of reheating respectively, as a function of n_s for three different values of X_0 for inverse cosh potential. Here vertical light pink region represents Planck bounds on n_s and dark pink region represents a precision of 10^{-3} from future experiments [42]. Horizontal dark purple region represents T_{re} of 10MeV from BBN and light purple region represents 100GeV of electroweak scale. Red dotted line corresponds to $w_{re} = -\frac{1}{3}$, blue dashed line corresponds to $w_{re} = 0$, green solid line corresponds to $w_{re} = 0.25$ and black dotdashed line corresponds to $w_{re} = 1$. For $X_0 = 7$ both N_{re} and T_{re} lie outside the Planck bound.

It can be seen from Table. I that for physically plausible values of w_{re} i.e between 0 and 0.25 the number of efolds should have values between $N_k = 46$ to $N_k = 55$. If we consider $w_{re} \leq 1$, we can allow N_k to be around 67. These upper bounds on N_k and n_s can be transferred into lower bounds on tensor-to-scalar ratio r .

The tensor-to-scalar ratio (22) for this model can be obtained from Eqs. (35) and (40) in terms of N_k as

X_0	Equation of state during reheating	n_s	N_k
7	$0 \leq w_{re} \leq 0.25$	$0.945 \leq n_s \leq 0.949$	$46.4 \leq N_k \leq 54.7$
	$0.25 \leq w_{re} \leq 1$	$0.949 \leq n_s \leq 0.954$	$54.7 \leq N_k \leq 67.0$
10	$0 \leq w_{re} \leq 0.25$	$0.954 \leq n_s \leq 0.959$	$46.5 \leq N_k \leq 54.9$
	$0.25 \leq w_{re} \leq 1$	$0.959 \leq n_s \leq 0.966$	$54.9 \leq N_k \leq 67.4$
15	$0 \leq w_{re} \leq 0.25$	$0.956 \leq n_s \leq 0.963$	$46.6 \leq N_k \leq 54.9$
	$0.25 \leq w_{re} \leq 1$	$0.963 \leq n_s \leq 0.969$	$54.9 \leq N_k \leq 67.4$
20	$0 \leq w_{re} \leq 0.25$	$0.957 \leq n_s \leq 0.963$	$46.6 \leq N_k \leq 54.9$
	$0.25 \leq w_{re} \leq 1$	$0.963 \leq n_s \leq 0.970$	$54.9 \leq N_k \leq 67.5$

TABLE I: The allowed values of spectral index n_s and number of efolds N_k for various values of X_0 for inverse cosh potential considering $T_{re} \geq 100\text{GeV}$.

$$r = \frac{16}{X_0^2} \left(\frac{1}{\sinh\left(\frac{2N_k}{X_0^2}\right)} \right), \quad (48)$$

and the spectral index can also be expressed in terms of N_k by inverting Eq. (46) as

$$n_s = 1 - \frac{2}{X_0^2} \frac{1}{\tanh\frac{N_k}{X_0^2}}. \quad (49)$$

The predictions for r and n_s can be obtained for various values of X_0 and N_k using Eqs. (48) and (46) for the potential Eq. (34). Fig. 2 shows N_k and r as a function of n_s corresponding to different values of equation of state during reheating w_{re} along with joint 68%CL and 95%CL Planck-2015 constraints. It can be seen from Fig. 2 that the physically plausible value of the equation of state $0 \leq w_{re} \leq 0.25$, which corresponds to $46 \leq N_k \leq 55$ is disfavored by Planck observations and w_{re} for these models should be close to 1 to satisfy Planck constraints on r and n_s for any value of X_0 . For n_s - r predictions of tachyon inflation with inverse cosh potential to fall within Planck-2015 1σ bounds, one requires the equation of state w_{re} to be larger than 1, which violates causality.

4.2. Exponential potential

Another string theory motivated potential for tachyon inflation is the exponential potential (3), which was studied by [39, 40]. In terms of variable $x \equiv \frac{T}{T_0}$ it can be expressed as

$$V(x) = \lambda e^{-x} \quad (50)$$

The slow-roll parameters for this model can be expressed using Eqs. (17) and (18) as

$$\epsilon_1 = \frac{\epsilon_2}{2} = \frac{1}{2X_0^2} e^x. \quad (51)$$

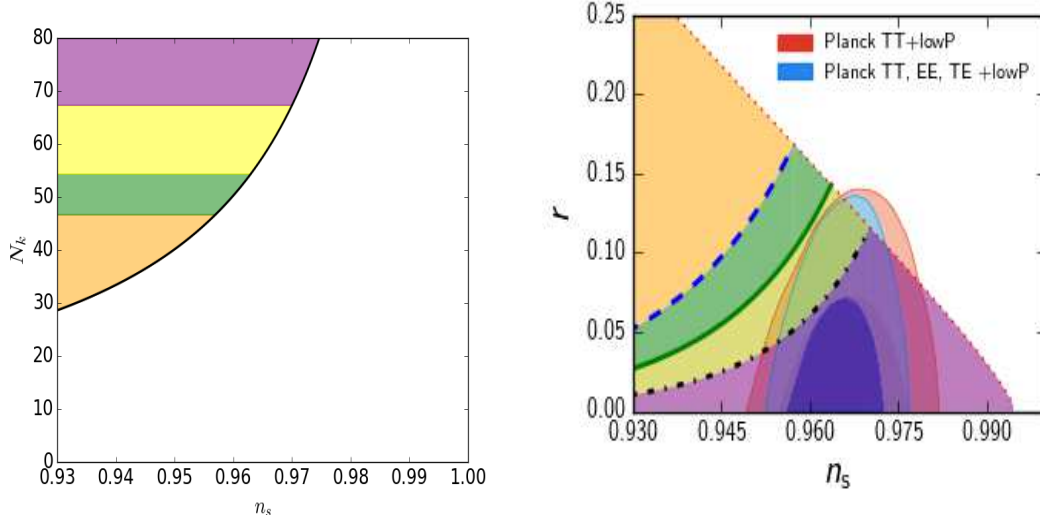


FIG. 2: N_k vs n_s and r vs n_s predictions for inverse cosh potential along with joint 68%CL and 95%CL Planck-2015 constraints. In both figures the orange region corresponds to $w_{re} < 0$, the green region corresponds to $0 < w_{re} < 0.25$, the yellow region corresponds to $0.25 < w_{re} < 1$ and the purple region corresponds to $w_{re} > 1$. In second figure dashed blue lines corresponds to $N_k = 46$, solid green lines corresponds to $N_k = 55$ and dashdotted black lines corresponds to $N_k = 67$.

To find the value of tachyon field at the end of inflation we put $\epsilon_1 = 1$ and we get

$$x_{end} = \ln(2X_0^2) \quad (52)$$

Using Eq. (38) the number of e-foldings N_k for this potential can be obtained as

$$N_k = X_0^2 = (e^{-x_k} - e^{-x_{end}}) = X_0^2 = \left(e^{-x_k} - \frac{1}{2X_0^2} \right) \quad (53)$$

One can see from this equation that $X_0^2 \geq (N_k + \frac{1}{2}) \geq N_k$. This is in contrast to the inverse cosh potential, where sufficient number of e-foldings can be obtained with any value of X_0 . The value of the tachyon field at the time when the mode k leaves the inflationary horizon can be obtained using Eq. (53) as

$$x_k = \ln \frac{X_0^2}{N_k + \frac{1}{2}}. \quad (54)$$

The spectral index n_s for this model is expressed using Eqs. (21) and (51) as

$$n_s = 1 - \frac{2}{X_0^2} e^{x_k}, \quad (55)$$

The relation between n_s and N_k can be obtained using Eqs. (54) and (55) as

$$N_k = \frac{2}{1 - n_s} - \frac{1}{2}. \quad (56)$$

The value of the potential at the end of inflation for this case can be expressed as

$$V_{end} = \lambda e^{-x_{end}} = 3M_p^2 H_k^2 \frac{e^{-x_{end}}}{e^{-x_k}}, \quad (57)$$

which using Eqs. (52) and (55) becomes

$$V_{end} = \frac{3}{4} M_p^2 H_k^2 (1 - n_s). \quad (58)$$

Hubble constant at time of horizon exit of mode k can be expressed in terms of scalar amplitude A_s and spectral index n_s using Eqs. (19,51,55) as

$$H_k = \pi M_p \sqrt{4A_s (1 - n_s) \left(1 - \frac{1}{12} (1 - n_s)\right)}. \quad (59)$$

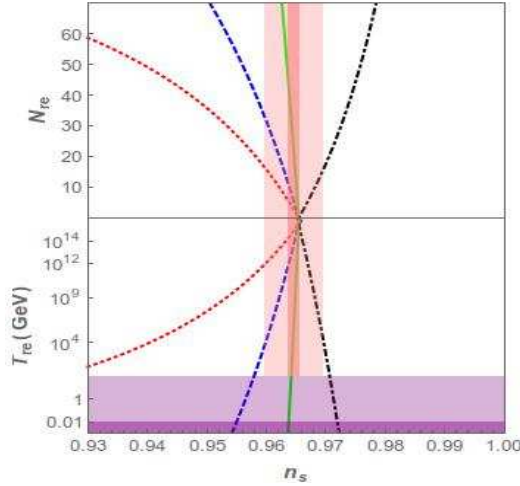


FIG. 3: Figure shows N_{re} and T_{re} , the length of reheating and temperature at the end of reheating respectively, as a function of n_s for exponential potential. Here all curves and shaded regions are same as Fig: 1.

Again for the potential (50), N_k , V_{end} and H_k are expressed in terms of A_s and n_s and one can obtain the temperature at the end of reheating T_{re} and the number of efolds during reheating N_{re} as a function of n_s using Eqs. (32) and (33), which are shown in Fig. 3. As in the case of inverse cosh potential we have again chosen four values of w_{re} between $-\frac{1}{3}$ to 1. For the physically plausible value of w_{re} i.e. $0 \leq w_{re} \leq 0.25$ and $T_{re} \geq 100\text{GeV}$, the value of n_s is restricted between $0.958 \leq n_s \leq 0.964$. This again corresponds to $47 \leq N_k \leq 55$. If we chose $0 \leq w_{re} \leq 1$, it can be seen from the Fig. 3 that $0.958 \leq n_s \leq 0.971$ for $T_{re} \geq 100\text{GeV}$, which gives $47 \leq N_k \leq 68$.

The tensor-to-scalar ratio (22) for this potential is given as

$$r = \frac{8e^{x_k}}{X_0^2} = 4(1 - n_s), \quad (60)$$

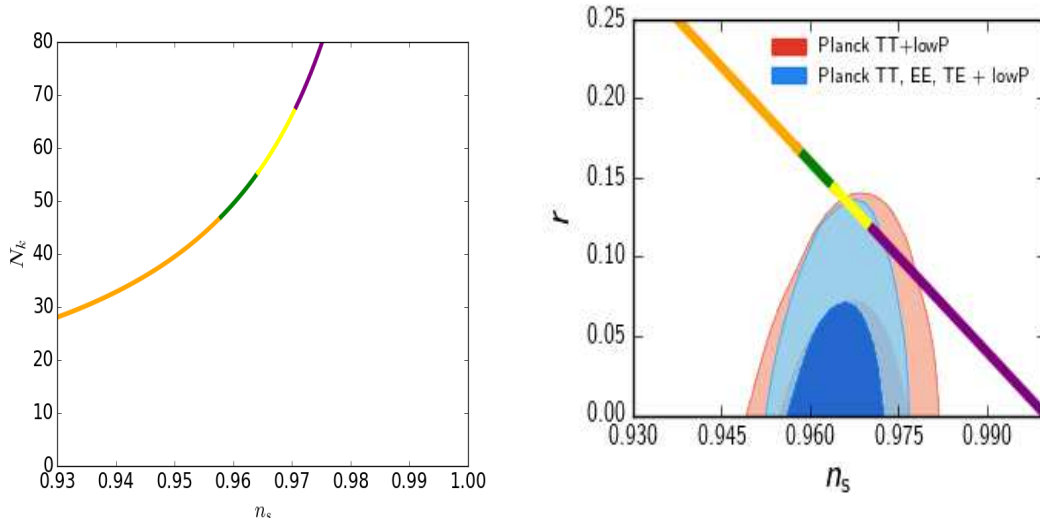


FIG. 4: N_k vs n_s and r vs n_s predictions for exponential inflation along with joint 68%CL and 95%CL Planck-2015 constraints. In both the figures orange portion of the curve represents allowed r and n_s for $w_{re} < 0$, green portion corresponds to w_{re} between 0 and 0.25, yellow portion corresponds to w_{re} between 0.25 and 1 and purple portion corresponds to $w_{re} > 1$. It can be seen from the figure that this model is ruled out by Planck observations at 2σ for physically allowed equation of state during reheating $0 \leq w_{re} \leq 0.25$.

where we have used Eq. (55) in the last step. The plots for N_k and r as a function of n_s are shown along with joint 68%CL and 95%CL Planck-2015 constraints in Fig. 4. The bounds on n_s obtained by imposing the condition $0 \leq w_{re} \leq 0.25$ and $T_{re} \geq 100\text{GeV}$ provide bounds on r as $0.144 \leq r \leq 0.168$. If we consider the broader range for w_{re} i.e. $0 \leq w_{re} \leq 1$, the bounds on r become $0.116 \leq r \leq 0.168$, which is slightly above than the Planck 2015 bound $r \leq 0.1$ [7]. As depicted in Fig. 4, the effective equation of state during reheating w_{re} for this choice of potential should lie between 0.25 and 1 to satisfy Planck constraints on r - n_s . Hence tachyon inflation with exponential potential (50) is disfavored if physically plausible value of reheating equation of state $0 \leq w_{re} \leq 0.25$ is considered.

5. CONCLUSIONS

Tachyon inflation [10–17] is one of the most attractive models of K -inflation [8, 9] motivated by string theory. In this work we have analyzed tachyon inflation by imposing constraints from reheating. This technique was earlier used to constrain various models of canonical inflation [35–37]. Here we chose inverse cosh potential [11, 12, 38] and exponential potential [39, 40] for our analysis. We compute reheating temperature T_{re} and number of e-folds during reheating N_{re} as a function of spectral index n_s for these potentials by assuming the effective equation of state during reheating w_{re} to be constant. w_{re} was obtained for various reheating scenarios [34] and it was found that $0 \leq w_{re} \leq 0.25$. By demanding $0 \leq w_{re} \leq 0.25$ and $T_{re} \geq 100\text{GeV}$ we find bounds on n_s and number of e-folds N_k from the time when mode k corresponding to pivot scale $k_0 = 0.05\text{Mpc}^{-1}$ leaves inflationary horizon

to the end of inflation. These bounds restrict the allowed regions in n_s - r plane for these potential.

For inverse cosh potential (2), as shown in Fig. 2, we find that N_k should lie between 46 and 55 for $0 \leq w_{re} \leq 0.25$. If we choose a broader range $0 \leq w_{re} \leq 1$, N_k can lie between 46 and 67. The n_s - r predictions for inverse cosh potential lie outside the Planck-2015 bounds for physically plausible values $0 \leq w_{re} \leq 0.25$.

For exponential potential (3), the condition $0 \leq w_{re} \leq 0.25$ and $T_{re} \geq 100\text{GeV}$ gives bounds on n_s as $0.958 \leq n_s \leq 0.964$, which corresponds to $47 \leq N_k \leq 55$. For $0 \leq w_{re} \leq 1$ we obtain $47 \leq N_k \leq 68$. As shown in Fig. 4, for this model also, the n_s - r predictions lie outside the Planck-2015 bounds for $0 \leq w_{re} \leq 0.25$. We also find that $r \geq 0.116$ for this model for $w_{re} \leq 1$, which is slightly higher than the Planck bound $r \leq 0.1$ [7]. Both exponential potential and inverse cosh potential are disfavored by Planck-2015 bounds on n_s - r for the physically plausible values of effective equation of state during reheating $0 \leq w_{re} \leq 0.25$. For both these models w_{re} close to 1 is required to satisfy Planck bounds on n_s and r . With tachyon potentials derived from string theory reheating is not well understood [43]. So this work can be helpful in determining correct mechanism for reheating in tachyon inflation.

-
- [1] A. H. Guth, Phys. Rev. D **23**, 347 (1981). doi:10.1103/PhysRevD.23.347
 - [2] V. F. Mukhanov and G. V. Chibisov, JETP Lett. **33**, 532 (1981).
 - [3] A. A. Starobinsky, Phys. Lett. **B117**, 175 (1982).
 - [4] A. H. Guth and S.-Y. Pi, Phys. Rev. **D32**, 1899 (1985).
 - [5] G. F. Smoot, C. L. Bennett, A. Kogut, E. L. Wright, J. Aymon, N. W. Boggess, E. S. Cheng, G. De Amici *et al.*, Astrophys. J. **396**, L1-L5 (1992).
 - [6] E. Komatsu *et al.* [WMAP Collaboration], Astrophys. J. Suppl. **192**, 18 (2011). [arXiv:1001.4538 [astro-ph.CO]].
 - [7] P. A. R. Ade *et al.* [Planck Collaboration], Astron. Astrophys. **594**, A20 (2016) doi:10.1051/0004-6361/201525898 [arXiv:1502.02114 [astro-ph.CO]].
 - [8] C. Armendariz-Picon, T. Damour, V. F. Mukhanov, Phys. Lett. **B458**, 209-218 (1999). [hep-th/9904075].
 - [9] J. Garriga, V. F. Mukhanov, Phys. Lett. **B458**, 219-225 (1999). [hep-th/9904176].
 - [10] G. W. Gibbons, Phys. Lett. B **537**, 1 (2002) doi:10.1016/S0370-2693(02)01881-6 [hep-th/0204008].
 - [11] A. Sen, JHEP **9910**, 008 (1999) doi:10.1088/1126-6708/1999/10/008 [hep-th/9909062].
 - [12] M. R. Garousi, Nucl. Phys. B **584**, 284 (2000) doi:10.1016/S0550-3213(00)00361-8 [hep-th/0003122].
 - [13] E. A. Bergshoeff, M. de Roo, T. C. de Wit, E. Eyras and S. Panda, JHEP **0005**, 009 (2000) doi:10.1088/1126-6708/2000/05/009 [hep-th/0003221].
 - [14] J. Kluson, Phys. Rev. D **62**, 126003 (2000) doi:10.1103/PhysRevD.62.126003 [hep-th/0004106].
 - [15] A. Sen, Int. J. Mod. Phys. A **18**, 4869 (2003) doi:10.1142/S0217751X03015313 [hep-th/0209122].
 - [16] D. Kutasov and V. Niarchos, Nucl. Phys. B **666**, 56 (2003) doi:10.1016/S0550-3213(03)00498-

- X [hep-th/0304045].
- [17] K. Okuyama, JHEP **0305**, 005 (2003) doi:10.1088/1126-6708/2003/05/005 [hep-th/0304108].
 - [18] A. Sen, JHEP **0204**, 048 (2002) doi:10.1088/1126-6708/2002/04/048 [hep-th/0203211].
 - [19] A. V. Frolov, L. Kofman and A. A. Starobinsky, Phys. Lett. B **545**, 8 (2002) doi:10.1016/S0370-2693(02)02582-0 [hep-th/0204187].
 - [20] L. Kofman and A. D. Linde, JHEP **0207**, 004 (2002) doi:10.1088/1126-6708/2002/07/004 [hep-th/0205121].
 - [21] D. A. Steer and F. Vernizzi, Phys. Rev. D **70**, 043527 (2004) doi:10.1103/PhysRevD.70.043527 [hep-th/0310139].
 - [22] N. Barbosa-Cendejas, J. De-Santiago, G. German, J. C. Hidalgo and R. R. Mora-Luna, JCAP **1803**, no. 03, 015 (2018) doi:10.1088/1475-7516/2018/03/015 [arXiv:1711.06693 [astro-ph.CO]].
 - [23] R. Allahverdi, R. Brandenberger, F. Y. Cyr-Racine and A. Mazumdar, Ann. Rev. Nucl. Part. Sci. **60**, 27 (2010) doi:10.1146/annurev.nucl.012809.104511 [arXiv:1001.2600 [hep-th]].
 - [24] L. F. Abbott, E. Farhi and M. B. Wise, Phys. Lett. **117B**, 29 (1982). doi:10.1016/0370-2693(82)90867-X
 - [25] A. D. Dolgov and A. D. Linde, Phys. Lett. **116B**, 329 (1982). doi:10.1016/0370-2693(82)90292-1
 - [26] A. Albrecht, P. J. Steinhardt, M. S. Turner and F. Wilczek, Phys. Rev. Lett. **48**, 1437 (1982). doi:10.1103/PhysRevLett.48.1437
 - [27] J. H. Traschen and R. H. Brandenberger, Phys. Rev. D **42**, 2491 (1990). doi:10.1103/PhysRevD.42.2491
 - [28] A. D. Dolgov and D. P. Kirilova, Sov. J. Nucl. Phys. **51**, 172 (1990) [Yad. Fiz. **51**, 273 (1990)].
 - [29] L. Kofman, A. D. Linde and A. A. Starobinsky, Phys. Rev. Lett. **73**, 3195 (1994) doi:10.1103/PhysRevLett.73.3195 [hep-th/9405187].
 - [30] L. Kofman, A. D. Linde and A. A. Starobinsky, Phys. Rev. D **56**, 3258 (1997) doi:10.1103/PhysRevD.56.3258 [hep-ph/9704452].
 - [31] B. R. Greene, T. Prokopec and T. G. Roos, Phys. Rev. D **56**, 6484 (1997) doi:10.1103/PhysRevD.56.6484 [hep-ph/9705357].
 - [32] J. F. Dufaux, G. N. Felder, L. Kofman, M. Peloso and D. Podolsky, JCAP **0607**, 006 (2006) doi:10.1088/1475-7516/2006/07/006 [hep-ph/0602144].
 - [33] G. N. Felder, L. Kofman and A. D. Linde, Phys. Rev. D **59**, 123523 (1999) doi:10.1103/PhysRevD.59.123523 [hep-ph/9812289].
 - [34] D. I. Podolsky, G. N. Felder, L. Kofman and M. Peloso, Phys. Rev. D **73**, 023501 (2006) doi:10.1103/PhysRevD.73.023501 [hep-ph/0507096].
 - [35] L. Dai, M. Kamionkowski and J. Wang, Phys. Rev. Lett. **113**, 041302 (2014) doi:10.1103/PhysRevLett.113.041302 [arXiv:1404.6704 [astro-ph.CO]].
 - [36] J. B. Munoz and M. Kamionkowski, Phys. Rev. D **91**, no. 4, 043521 (2015) doi:10.1103/PhysRevD.91.043521 [arXiv:1412.0656 [astro-ph.CO]].
 - [37] J. L. Cook, E. Dimastrogiovanni, D. A. Easson and L. M. Krauss, JCAP **1504**, 047 (2015) doi:10.1088/1475-7516/2015/04/047 [arXiv:1502.04673 [astro-ph.CO]].
 - [38] N. D. Lambert, H. Li and J. M. Maldacena, JHEP **0703**, 014 (2007) doi:10.1088/1126-6708/2007/03/014 [hep-th/0303139].
 - [39] A. Sen, Mod. Phys. Lett. A **17**, 1797 (2002) doi:10.1142/S0217732302008071 [hep-th/0204143].

- [40] M. Sami, P. Chingangbam and T. Qureshi, Phys. Rev. D **66**, 043530 (2002) doi:10.1103/PhysRevD.66.043530 [hep-th/0205179].
- [41] D. J. Schwarz, C. A. Terrero-Escalante and A. A. Garcia, Phys. Lett. B **517**, 243 (2001) doi:10.1016/S0370-2693(01)01036-X [astro-ph/0106020].
- [42] L. Amendola *et al.*, Living Rev. Rel. **21**, no. 1, 2 (2018) doi:10.1007/s41114-017-0010-3 [arXiv:1606.00180 [astro-ph.CO]].
- [43] J. M. Cline, H. Firouzjahi and P. Martineau, JHEP **0211**, 041 (2002) doi:10.1088/1126-6708/2002/11/041 [hep-th/0207156].